Depolarization of Cellular Resting Membrane Potential Promotes Neonatal Cardiomyocyte Proliferation In Vitro

Jen-Yu Lan[1], **Corin Williams**[1], **Michael Levin**[2,3], and **Lauren Deems Black III**[1,4]

[1]Department of Biomedical Engineering, Tufts University, Medford, MA 02155 USA

[2]Department of Biology, Tufts University, Medford, MA 02155 USA

[3]Center for Regenerative and Developmental Biology, Tufts University, Medford, MA 02155 USA

[4]Cellular, Molecular and Developmental Biology Program, Sackler Graduate School of Biomedical Sciences, Tufts University School of Medicine, Boston, MA 02111 USA

Abstract

Cardiomyocytes (CMs) undergo a rapid transition from hyperplastic to hypertrophic growth soon after birth, which is a major challenge to the development of engineered cardiac tissue for pediatric patients. Resting membrane potential (V_{mem}) has been shown to play an important role in cell differentiation and proliferation during development. We hypothesized that depolarization of neonatal CMs would stimulate or maintain CM proliferation *in vitro*. To test our hypothesis, we isolated postnatal day 3 neonatal rat CMs and subjected them to sustained depolarization via the addition of potassium gluconate or Ouabain to the culture medium. Cell density and CM percentage measurements demonstrated an increase in mitotic CMs along with a ~2 fold increase in CM numbers with depolarization. In addition, depolarization led to an increase in cells in G2 and S phase, indicating increased proliferation, as measured by flow cytometry. Surprisingly depolarization of V_{mem} with either treatment led to inhibition of proliferation in cardiac fibroblasts. This effect is abrogated when the study was carried out on postnatal day 7 neonatal CMs, which are less proliferative, indicating that the likely mechanism of depolarization is the maintenance of the proliferating CM population. In summary, our findings suggest that depolarization maintains postnatal CM proliferation and may be a novel approach to encourage growth of engineered tissue and cardiac regeneration in pediatric patients.

Keywords

Cell cycle; potassium gluconate; ouabain; Cardiac Fibroblasts; Akt pathway

Address for Correspondence: Lauren Deems Black III Department of Biomedical Engineering Tufts University 4 Colby Street Medford, MA 02155 Ph: (617) 627-4660 Fx: (617) 627-3231 lauren.black@tufts.edu.

Introduction

Congenital heart defects (CHDs) occur with a prevalence of 8 per 1000 live births [1] and are the leading cause of mortality in live-born infants and young children. Hypoplastic left heart syndrome (HLHS) is a CHD that involves the underdevelopment of the left ventricle, and it is lethal unless there is prompt surgical intervention soon after birth. In the 1980s, the development of a series of surgeries to create a uni-ventricular heart from the right ventricle led to significantly improved survival of HLHS patients in the decades since [2]. However, many of these patients continue to suffer from secondary complications throughout life, including heart failure at a young age, for which the only long-term option is heart transplantation. As such, there is a need to develop novel strategies for treating these young patients in a way that can recapitulate or restore healthy heart anatomy and function. Of note, recent studies in animal models have pointed to decreased cardiomyocyte (CM) proliferation in the developing heart as a potential mechanism for HLHS [3]. Thus, targeting CM proliferation could be a potentially powerful strategy for encouraging growth and function of the underdeveloped left ventricle in the young HLHS patient.

A major challenge to cardiac regeneration in general is the conception that CMs transition from hyperplastic to hypertrophic growth soon after birth [4]. Indeed, postnatal mammalian CMs were previously considered to be terminally differentiated and thus non-proliferative, with postnatal increases in heart size and function mainly attributed to CM hypertrophy with increasing age. Recently, scientists have discovered a significant capacity for cardiac regeneration in other vertebrate species, such as zebrafish [5] and newt [6], and it has also been demonstrated that the neonatal mouse heart has a transient capability of regeneration, which diminishes after postnatal day 7 [7]. Even more striking was the finding that cardiomyocyte proliferation plays an important role in heart growth before age 20 in humans [8]. Thus, it may be inferred that CMs have intrinsic potential for proliferation, but this capability is strongly down-regulated as the cells mature.

Although growth factors, cell-cell signaling, mechanical cues, and extracellular matrix [9, 10] have been shown to affect cell proliferation, the role of bioelectrical signaling has in the past been largely overlooked. More recently, a significant body of literature has demonstrated that endogenous bioelectric signals play a role in controlling limb and spinal cord regeneration [11], cell and embryo polarity [12], proliferation [13] and migration guidance [14] of numerous cell types. Pioneering work by Clarence Cone in the late 60′s and early 70′s demonstrated the role of resting membrane potential (V_{mem}) in cellular proliferation [15]. Of particular significance, he demonstrated that mature neurons from the central nervous system (typically thought of as terminally differentiated and thus non-mitotic) could be stimulated to proliferate by sustained depolarization of V_{mem} via pharmacological treatments [16]. More recently, it was found that human mesenchymal stem cells (hMSCs) could be driven to differentiate via hyperpolarization while depolarization maintained the stem cell phenotype, and that a degree of de-differentiation can be obtained in differentiated hMSCs by manipulation of their resting potential [17]. It is generally accepted that stem cells are significantly more proliferative than differentiated cell types [18, 19], and thus these studies suggest an intriguing link between V_{mem} and a switch from a

proliferative to mature state. However, no one has investigated the effect of alterations to V_{mem} on the proliferative behavior of CMs.

The goals of this study were to assess CM proliferation in response to alterations in V_{mem}, and to determine the possible signaling pathways activated by depolarization. Sustained depolarization of cardiac cells isolated from postnatal day 3 (P3) and postnatal day 7 (P7) rat hearts was carried out by the addition of potassium gluconate or ouabain to the culture medium at a range of concentrations. Quantitative analysis of immunohistochemical staining of cell populations indicated increased CM numbers in response to depolarization. Interestingly, proliferation of cardiac fibroblasts (CFs) was inhibited with either treatment, independent of the concentration. Cell cycle analysis using flow cytometry confirmed alterations in the mitotic population of cells that correlated with cell counts. Growth signaling pathways were also studied via Western blot and showed increased activation of the ERK-MAPK pathway in treated cells. Our findings indicate that depolarization of CMs results in increased CM proliferation and may serve as a potentially powerful tool for cardiac regeneration and repair in pediatric patients suffering from CHDs

Materials and Methods

Cell isolation and culture

All procedures involving animals were carried out in accordance with the Institutional Animal Care and Use Committee at Tufts University and the NIH Guide for the Care and Use of Laboratory Animals. Briefly, Sprague Dawley rat pups at either P3 or P7 were euthanized by conscious decapitation and the hearts were harvested. After removal of the atrial tissue, ventricles were minced and subjected to a series of digestions with type II collagenase (Worthington Biochemical Corp, Lakewood, NJ) as previously described [10]. Cardiac fibroblasts (CFs) were obtained by the pre-plate method [20] and utilized on the second passage.

Treatments to alter membrane potential

Primary cardiac cells (mixed population of CMs and CFs) from either P3 or P7 rats were seeded at an initial density of $1.0 \times 10^5/cm^2$ and cultured for one day in Myo Media (10% horse serum, 2% fetal bovine serum, and 1% penicillin-streptomycin in Dulbecco's Modified Eagle Medium; all from Invitrogen). The wells were then divided into one of three groups. The control group was given fresh Myo Media without the addition of any supplements. The other two groups were subjected to sustained depolarization with the addition of either potassium gluconate or ouabain. To assess dose dependent effects, we studied a range of concentrations for both potassium gluconate (5 mM, 10 mM, 20 mM, 40 mM, 60 mM, and 80 mM) and ouabain (10 nM, 100 nM, 1 μM, 10 μM, 100 μM, and 150 μM) , reagents known to depolarize V_{mem} [16, 17, 21-27]. Sustained depolarization was carried out for 72 hours with no media change. CFs from P3 rats were also subjected to depolarization to determine the independent effects on mitosis for this specific cell population. Cells were assessed at day 4 of culture using the methods described below.

Membrane potential measurements

To verify that both treatments led to alterations in resting cell membrane potential, the voltage sensitive dye Bis-(1,3-dibutylbarbituric acid)-trimethine oxonol (DiBAC4(3)) was used [28-30]. Briefly, a stock solution was prepared at a concentration of 2 mM and diluted 1:4000 [28] in the media described above. Fluorescent images were obtained for each of the groups described above using an Olympus IX81 microscope (Olympus America, Chelmsford, Massachusetts) equipped with Metamorph Basic software (version 7.7.4.0, Molecular Devices, Sunnyvale, CA) and subsequently analyzed in ImageJ (v1.45s, NIH, Bethesda, MD). Fluorescence intensity ratio was measured as the cell membrane fluorescence intensity divided by the background intensity. A minimum of 149 cells per condition was measured. The ratio reflects the relative membrane potential with a larger ratio corresponding to a more depolarized membrane.

Immnunocytochemistry

After 4 days in culture, the cells were washed with PBS and fixed with ice cold 100% methanol for 10 min (n = 8 wells for each condition). The samples were blocked with 5% donkey serum and then incubated with a mouse monoclonal cardiac-specific α-actin antibody (sc-58670, Santa Cruz Biotechnology, Dallas, Texas) and a rabbit polyclonal phospho-histone H3 (PHH3) antibody (sc-8656-R, Santa Cruz Biotechnology), to identify CMs and proliferating cells, respectively. A rabbit anti-actinin antibody (ab147436, Abcam, Cambridge, Massachusetts) was used for sarcomeric length measurement. Cy3 donkey anti-mouse antibody (Jackson ImmunoResearch, West Grove, Pennsylvania) and Alexa Fluor 488 donkey anti-rabbit antibody (Jackson ImmunoResearch) were used as secondary antibodies, respectively. Hoechst 33342 (Invitrogen, Carlsbad, California) was used to stain cell nuclei. The samples were then imaged (n=4 images per well, thus 32 images for each condition) and analyzed as described below.

Quantification of total cell, CM and CF numbers

The quantification of immunohistochemical images was carried out using ImageJ. The total number of nuclei per cm^2 was determined using images of the Hoechst stain. Assessment of CM number was carried out by creating a mask of the regions of cardiac α-actin stain, applying this mask to the images of the Hoechst stain and counting the number of nuclei contained within the masked regions (see Figure 1 for example images). CF number in response to treatment was assessed by total nuclear counts on P3 CFs cultured under the conditions described above.

Cell cycle analysis

To determine whether depolarization resulted in changes to the number of cells entering the cell cycle, we used flow cytometry to investigate the DNA content of cells in control and treatment conditions. Briefly, cells were trypsinized, fixed with 70% ethanol, washed with PBS and resuspended in staining buffer (100 mM Tris, pH 7.4, 150 mM NaCl, 1 mM CaCl2, 0.5 mM MgCl2, 0.1% Nonidet P-40) containing Ribonuclease A to prevent RNA staining (final concentration of 100 μg/mL, cat # 19101, Qiagen, Venlo, Netherlands) and propidium iodide (final concentration of 2 μg/mL, cat # P3566, Invitrogen, Carlsbad, California) and

incubated for 15 minutes at room temperature at a cell concentration of 1.0×10^6/mL. Flow cytometry was carried out with a FACS Calibur system (BD Biosciences, San Jose, California). 10,000 events per sample were counted with appropriate gates to exclude cell aggregates and debris according to the FL2-W channel. Cell cycle analysis was carried out using FlowJo software (TreeStar Inc., Ashland, Oregon). The cell cycle phases were fit to the Dean-Jett-Fox cell cycle modeling algorithm [31].

Western blot analysis

In order to assess the potential cell signaling pathways involved in any measured effect of depolarization, we identified pathways previously implicated in proliferation and cell survival and studied them using Western blot techniques previously described by our lab [32]. Briefly, after the 4 days in culture cells were lysed and analyzed with a BCA assay (Pierce, Rockford, Illinois) to determine the protein concentration for each sample. Equal amounts of protein (25 μg per lane) were loaded into pre-cast 4-15% polyacrylamide gels (cat # 456-1086, BioRad, Hercules, California) and SDS-PAGE was carried out before the resulting gel was transferred to a PVDF membrane (Millipore). The blot was blocked with 5% Carnation milk in Tris Buffered Saline containing 0.1% Tween20 and then labeled with antibodies for proteins of interest. The following primary antibodies were used with 1:1000 dilutions: Akt1 (cat # 2938S), panAkt (cat #4685S), phosphorylated ERK1/2 (cat # 9101S), ERK1/2 (cat # 4695S), phosphorylated MEK1/2 (cat # 2338S), and MEK1/2 (cat # 9122S, all from Cell Signaling Technology, Danvers, Massachusetts), and GAPDH as a loading control (G-9575 Sigma, St. Louis, Missouri). Species-specific secondary antibodies conjugated to HRP (cat #s 656120 and 656520, Invitrogen, Carlsbad, California) were used for enhanced chemiluminescence. The blot was then imaged by a G:Box Chemi XR5 (Syngene, Cambridge, UK). Data presented are normalized to the expression of the control population to demonstrate fold changes in expression.

Statistical Analysis

All data are presented as mean ± standard deviation (SD). Experimental data was statistically compared via one way ANOVA (treatment concentration) with a Student's t-test method for posthoc testing of treatment group to control group comparisons. Statistical significance was determined as $p<0.05$.

Results

Validation of Depolarization

DiBAC staining of mixed P3 cardiac cell populations demonstrated an increase in the intensity ratio with increasing concentrations of both potassium gluconate and ouabain (Figure 2 and b, respectively) up to an optimal concentration (40 mM for potassium gluconate and ~10μM for ouabain). Further increases in the concentration of the depolarizing agents above these levels led to subsequent decreases in the intensity ratio. Note that the intensity ratio for the all concentrations of potassium gluconate was significantly higher than control values. Similarly, the fluorescence intensity ratio at 10 μM ouabain was significantly greater than control while those concentrations over the 10μM concentration of ouabain were significantly lower than control values ($p<0.05$). In addition,

it is important to note that the depolarization response of cells to potassium gluconate was much stronger than that in response to ouabain.

Direct Assessment of Proliferation in Cultures

To assess the effects of depolarization on the proliferation of cardiac cells, we labeled cells subjected to the various treatments with cardiac α-actin, PHH3 and Hoechst stain. Figure 3 shows representative images for the control (top), 40mM potassium gluconate (middle) and 10 μM Ouabain (bottom). Note that there is a qualitative increase in CM number (as denoted by the increased cardiac alpha-actin staining) with both treatments and PHH3 positive cells in the ouabain group. To quantify the proliferation within these cultures we used ImageJ to analyze the number of PHH3 positive cells and the number of PHH3 positive CMs in the P3 mixed culture. Supplemental Figure 1 shows the percentage of PHH3 positive cells for the total cell population (top row) and the percentage of PHH3 positive CMs (bottom row) for potassium gluconate (left column) and ouabain (right column). Note that there was an increase in PHH3 positive cells in both the total and CM specific populations with both treatments; however, there was no statistically significant difference between any of the treatment groups and the control condition.

CM and Total Cell Counts with Treatment

To further assess the effects of treatment on cell proliferation we studied total cell and CM number in both P3 and P7 mixed cardiac populations using the method described in Figure 1. For P3 cells (darker bars, Figure 4), both treatment groups showed a trend of slightly increasing total cell density at the middle of the range of concentration (40 mM for potassium gluconate and 10 μM for ouabain) before decreasing at higher concentrations (Figure 4 a, b). However, the effect of both depolarization agents on total cell number was not statistically significant. We also determined CM density and found that CMs were significantly increased compared to control conditions in the 20 mM, 40 mM and 60 mM potassium gluconate conditions, as well as at the 100 nM and 10 μM ouabain conditions (Figure 4c, d). CM density was also significantly reduced at the highest concentration of ouabain (150 μM). The percentage of CMs in culture followed similar trends to the CM density measures for potassium gluconate, showing a general trend of increasing CMs with increasing concentration, with the 40 mM, 60 mM and 80 mM concentrations having significantly higher CM percentage than the control condition (Figure 4e). In the ouabain treatment group, CM percentage was fairly similar across conditions with only the 10 μM concentration demonstrating a significant (albeit modest) increase and the 150 μM concentration demonstrating a rather steep and significant decrease as compared to control (Figure 4f).

We were next interested in determining if depolarization was maintaining a proliferative population of myocytes or stimulating proliferation. As the switch from hyperplasia to hypertrophic growth occurs around P3 in the rat [4], CM proliferation should be significantly reduced at P7 (lighter bars, Figure 4). Total nuclei numbers were fairly consistent with both of the depolarizing treatments in the P7 cardiac cells, significantly decreasing only at the highest doses of the two treatments (60 mM and 80mM of potassium gluconate and 150 μM ouabain, Figure 4a, b); however, the total CM density still

demonstrated a significant increase at 40 mM potassium gluconate (18475 ± 3081 CM/ cm^2 vs. 13083 ± 1859 CM/cm^2 for control condition) (Figure 4c, d). CM percentage increased with increasing concentration of potassium gluconate, with the 40 mM, 60 mM and 80 mM concentrations resulting in statistically significant increases (Figure 4e). There was no significant change in CM percentage at any concentration of ouabain (Figure 4f). In comparing results from P3 cells to those from P7 cells, it is clear that total cell density and CM density are significantly reduced at almost every condition, suggesting decreased proliferation in the P7 population. The exceptions to this are the total cell density at 40 mM potassium gluconate, which is not significantly different from P3 cells, and the CM density at 150 mM ouabain, which is significantly lower in the P3 case as compared to the P7 case. In contrast, CM percentage is the same for both P3 and P7 populations in all cases except for the control condition and the highest concentrations of each of the treatments (80 mM potassium gluconate and 150 μM ouabain) where the P7 values were significantly higher than the P3 values.

The growth curve for the optimal concentrations of both potassium gluconate (40 mM) and ouabain (10 μM) groups compared to the control group is plotted over the course of four days. To demonstrate any changes in the cell makeup of the mixed population with culture time, the percentage of CMs as a function of days in culture is shown in figure 5a. All of the groups demonstrate a decrease in CM percentage over the culture period. The control group decreases significantly at days 3 and 4 as compared to day 1. The potassium group has a slower drop in CM percentage that does not achieve significance until day 4, and remains significantly higher than the control group at both days 3 and 4. In the ouabain group, CM percentage significantly declines on day 3, but has a comparable percentage on day 4, and maintains a significantly higher percentage than the control group at the final time point. Although total CM count in the control group gradually increases with time, the CM count of both the potassium group and the ouabain group have a consistently steeper rise (Figure 5b).

Effects of Depolarization on Cardiac Fibroblasts

As depolarization did not significantly affect total cell numbers in the mixed cardiac cell population but did lead to increased CM numbers, we wondered if CF proliferation may be inhibited. To assess the effects of the depolarization treatments on the CF fraction of the mixed population, we subjected CFs isolated from P3 rats to the same treatments and analyzed total cell number. Representative images of the Hoechst nuclear stain demonstrated a reduction in cell number with either potassium gluconate or ouabain treatment (Figure 5a). Quantification of these images demonstrated that the addition of either potassium gluconate (Figure 5b) or ouabain (Figure 6c) to the culture medium significantly reduced the number of CFs in the culture ($p<0.05$). Compared to the day 1 time point, CF densities in all treatments are slightly increased, but the increase is significantly less than the approximately three fold increase of the control group. Furthermore, the reduction in CF number was not concentration dependent for either treatment, with even the lowest concentration of each of the depolarizing agents resulting in a greater than 50% decrease in cell number in all treatment groups compared to control.

Cell Cycle Analysis via FACS

To determine whether depolarization treatments were impacting cell cycle progression, cell cycle analysis was performed with propidium iodide to quantify the relative amount of DNA within cells in the mixed P3 cardiac cell populations (Figure 7). This analysis was carried out for cells in the control conditions as well as those in the optimal concentration of each of the treatments, defined as the condition with the greatest CM density (40 mM potassium gluconate and 10 μM ouabain). In the P3 whole population (mixed CMs and CFs), we found a decrease in the G0/G1 phase and an increase in the non-G0/G1 phase with both of the optimal treatments. Overall, the cell cycle analysis agreed well with the results of the image analysis methods.

Potential Pathways Involved in Response

To investigate the potential pathways involved in the response of the P3 cells to the depolarizing treatments, we used Western blot to study the Akt and MAPK/ERK pathways (Figure 8). For the potassium gluconate treated group we noted an increase in Akt1 with a comparable level of panAkt, but this was not significant. Both pERK1/2 and pMEK1/2 were significantly increased with potassium gluconate treatment while the overall level of ERK1/2 and MEK1/2 stayed the same. With the ouabain induced depolarization, Akt1 expression increased significantly, and panAkt stayed at the same level as the control group. Both pERK1/2 and pMEK1/2 demonstrated a strong enhancement in the treatment groups as compared with control group, while ERK1/2 and MEK1/2 were unchanged from control conditions.

Discussion

CHDs are the leading cause of mortality in live-born infants [33] and current strategies to repair them are palliative in nature, leading to a number of secondary complications throughout life and the eventual need for total heart transplantation in many young patients. Recent studies have indicated that decreased CM proliferation may be a potential mechanism for the progression of HLHS, a specific CHD resulting in the underdevelopment of the left ventricle. As such, strategies which promote the proliferation of CMs could have a significant impact on the treatment of CHDs such as HLHS. While many studies have focused on the use of substrate properties or growth factors to promotes CM proliferation [9, 10], the role of bioelectric potential in promoting CM proliferation has been left unexplored, even though it is known that V_{mem} is related to cellular differentiation state and that depolarization of another terminally differentiated cell type, neurons, promoted mitosis in these cells [34-38]. The goal of this study was to assess the effects of depolarization of V_{mem} on CM proliferation and to investigate the potential signaling pathways that may be involved. Our data demonstrate that treatment with either potassium gluconate or ouabain induced CM proliferation in P3 cells and inhibited CF mitosis, but that potassium gluconate produced a more pronounced response. This effect was still present, albeit blunted, at P7. Surprisingly, depolarization of V_{mem} with either treatment led to inhibition of proliferation in CFs. Cell cycle analysis via flow cytometry confirmed alterations in the mitotic population of the cells in response to treatment. Western blot analysis implicated the Akt

and MAPK/ERK pathways in the proliferative response of the cells to depolarizing treatments. The specific findings are discussed in more detail below.

In this study we used potassium gluconate and ouabain to depolarize cells. Potassium gluconate induces depolarization by altering the concentration difference of potassium across the cell membrane, while ouabain affects resting membrane potential by blocking the activity of the Na^+-K^+-ATPase channel. DIBAC4(3), a slow acting voltage-sensitive dye, was used to validate the depolarizing effects of each of these treatments at a range of concentrations. Previous studies have demonstrated the linearity between fluorescence intensity ratio and V_{mem} by patch clamping techniques [39], where a higher intensity ratio indicated increased depolarization of V_{mem}. Both the potassium gluconate and ouabain groups showed increased DiBAC(4)3 fluorescence intensity ratio with increasing concentration until some optimal level before further increases in concentration led to decreasing ratios (Figure 2). While the overall increases in fluorescence ratio were modest (particularly in the ouabain group), they were significant and resulted in qualitative and quantitative differences in CM number and PHH3 positive cells in the treated cultures (Figure 3, Supplemental Figure 1, Figure 4). Future work would involve further validation of the depolarization of V_{mem} via patch clamping. Moreover, this method would allow us to directly quantify the specific value of r V_{mem} that promoted the greatest degree of proliferation and thus give a target to aim for in the development of other methods to promote CM proliferation through this mechanism.

The crux of this work was centered on the premise that V_{mem} is linked to cell maturity and that alterations in V_{mem} can promote or maintain a proliferative phenotype in naturally maturing cell populations. Previously, Cone et al found that depolarization of mature neurons, previously considered a terminally differentiated cell type incapable of proliferation, led to mitosis [16]. Around the same time, a study measuring V_{mem} of cells undergoing mitosis demonstrated elevated membrane potential when entering S phase which declined again when entering mitosis [40], highlighting a potential link between mitosis and V_{mem}. In our study, the mitotic marker PHH3 was used initially to identify CM- specific and general cell mitosis (Supplemental Figure 1). In terms of the total cell population there was a trend of increased PHH3 positive cells with increasing dose in both treatment types, but this trend was not significant. In the control group, few PHH3 positive cells were also cardiac α-actin positive; however, there were conditions with increased percentage of PHH3 positive CMs in each of the treatment types. These values were not significantly different from control. One likely reason for the lack of statistically significant differences and the high variability in the PHH3 data is the low number of PHH3 positive cells in culture. PHH3 is only present at a specific point during mitosis and thus may not be capturing the full number of cells undergoing proliferation. Future work would involve studying other markers of proliferation such as Ki67 or BrdU.

To address the above issue with PHH3 variability, we quantified total cell and CM densities in the cultures to assess expansion with treatment (Figure 4). In general, P3 cells responded to both treatments by increasing the CM density with increasing dose up to an optimal concentration, before eventually decreasing. This led to significant increases in the percentage of CMs with increasing potassium, but there was no change to CM percentage

with ouabain other than a significant decrease at the highest concentration. Compared to P3, the P7 cell populations had lower total cell and CM densities but had similar percentage of CMs. Even though the density of more mature CMs was far less than that of younger CMs, depolarization still promoted proliferation *in vitro*, particularly at 40 mM potassium gluconate and 10 μM ouabain. Investigating these concentrations further, we carried out a growth curve analysis over the course of 4 days (Figure 5) and found that both groups had significantly higher rate of growth compared to the control group. Interestingly, the cardiac α-actin positive cells in the 40mM potassium gluconate group were well spread and polygonal shaped; however the cells in the ouabain group tended to cluster into colonies (Figure 3) indicating potentially differential effects on cell phenotype with the two treatments. However, there was no significant difference in sarcomere length, a measure of cardiomyocyte maturity [41], between any of the three groups (Supplemental Figure 2). It is important to note that quantifying proliferation via histological staining and cell counting, particularly in a mixed cell population, can be difficult and result in potential errors. Specifically, there is the possibility that CFs that are growing on top of CMs may inflate the CM number as the nucleus may still be counted as a CM nucleus. We have minimized this effect by only counting nuclei fully contained in the cardiac alpha actin stain mask and eliminating those where only part of the nucleus is in the mask. Moreover, we do not expect this type of error to be significant in magnitude given that the cultures are not over-confluent. Lastly, the error should be present in all conditions to the same degree and thus relative comparisons between groups will still be valid.

In our experience, CFs can be expanded quickly in culture, are easy to passage, and have high viability. As they make up a large fraction of the mixed cell population used in this study, we sought to investigate the effects of depolarization on the proliferation of the purified CF population. Interestingly, CF proliferation was inhibited with potassium gluconate or ouabain treatment (Figure 6). In the control group, the CFs grew over-confluent in 4 days, while both potassium and ouabain groups were at sub-confluent levels. This effect was relatively concentration independent. A number of studies have shown the effect of potassium and ouabain on fibroblasts. Nicorandil, an ATP sensitive potassium channel opener, was shown to inhibit the angiotensin-II induced proliferation of CFs [42]. Ouabain has demonstrated mixed effects with one study showing that is has a slight proliferative effect on CFs [43], while another study conducted at a lower range of concentration (similar to the range in our experiment) showed inhibition of proliferation with ouabain treatment [44]. The different proliferative responses of cardiomyocytes and fibroblasts to depolarizing agents may be due to distinct potassium channel profiles [45], but the exact mechanism will require further study. Taken together, these data demonstrate that even though the specific mechanism of the different responses of CMs and CFs to depolarization remain unclear, depolarization induced by either of the treatments had a proliferative effect on CMs, which was confirmed by flow cytometry-based assessment of cell cycle (Figure 7).

In order to assess the potential mechanism of the observed responses to depolarization, we used Western blot analysis to investigate the Akt and ERK/ MAPK signaling pathways. It was previously demonstrated that Akt promoted *in vitro* survival of CMs mediated by IGF-1, and enhanced cell cycling and cardiac progenitor cell expansion by nuclear-targeted

Akt transgenics [46]. In addition, Akt knockout led to heart defects and reduced proliferation [47]. Both potassium and ouabain have been reported to have effects on the Akt pathway. A previous study demonstrated that high extracellular potassium could promote neuron survival via the PI3/Akt pathway [48]. The effects of ouabain on hypertrophy in the heart via activation of the PI3K/ Akt pathway have also been widely studied [49]. In our experiment, we saw changes in Akt1 expression that mirrored the response of CMs to treatment in both groups. With regards to ERK, it has been demonstrated to promote CM survival, and could be activated by the GPCR, Ras/Raf cascade [50]. Indeed, potassium-induced depolarization activated ERK and proline-rich tyrosine kinase in the central nervous system [51, 52] and a similar result was also found in CMs treated with potassium channel blockers [53]. In our study, ERK 1/2 was fairly consistent across both treatment groups; however activated ERK (pERK1/2) is upregulated in both potassium and ouabain groups. Moreover, the activation of the upstream kinase, MEK1/2, likely explains the upregulation of ERK phosphorylation. It is important to note that ATPase could induce signal transduction via other modes besides the ion channel [54], and thus the signal transduction of ouabain may be more versatile and could be acting through other agents including growth factor signaling. Future work would be to further investigate this as a potential mechanism.

Conclusions

In summary, prolonged depolarization led to proliferation and cell cycle progression in CMs, but suppressed the growth of CFs. P7 cells were less proliferative than P3 but still demonstrated an increase in CM density in response to the depolarizing treatments. The Akt and MAPK pathways may be responsible for bridging the changes in bioelectric potential to cell proliferation. Although the detailed intracellular signaling pathway will require further studies, the data presented herein demonstrate that the manipulation of biopotential provides a novel approach to stimulate cell cycle progression and expansion of neonatal CMs, thus providing a potential therapeutic strategy for promoting cardiac regeneration in young patients suffering from CHDs.

Supplementary Material

Refer to Web version on PubMed Central for supplementary material.

Acknowledgments

Biography

Lauren D. Black III received his BS in Aerospace Engineering from the University of Cincinnati and a MS and PhD in Biomedical Engineering from Boston University. In his thesis work under Dr. Bela Suki, he studied the role of alterations in the structural protein composition of the extracellular matrix in static and dynamic mechanical properties of

tissues. He went on to a postdoctoral fellowship in the lab of Dr. Robert Tranquillo at the University of Minnesota, developing new tools to generate and culture engineered cardiac tissues. During his time in Minnesota he was awarded an F32 individual postdoctoral fellowship and a subsequent K99/R00 Pathway to Independence Award from the National Heart, Lung and Blood Institute at the National Institutes of Health. Dr. Black started as an Assistant Professor in the Biomedical Engineering Department at Tufts University in 2010, where he was recently awarded an NSF CAREER Award. His lab focuses on the role of extracellular biophysical signaling in normal and pathological cardiac development.

References

1. van der Linde D, Konings EE, Slager MA, Witsenburg M, Helbing WA, Takkenberg JJ, Roos-Hesselink JW. Birth prevalence of congenital heart disease worldwide: a systematic review and meta-analysis. Journal of the American College of Cardiology. 2011; 58(21):2241–2247. [PubMed: 22078432]

2. Feinstein JA, Benson DW, Dubin AM, Cohen MS, Maxey DM, Mahle WT, Pahl E, Villafane J, Bhatt AB, Peng LF, Johnson BA, Marsden AL, Daniels CJ, Rudd NA, Caldarone CA, Mussatto KA, Morales DL, Ivy DD, Gaynor JW, Tweddell JS, Deal BJ, Furck AK, Rosenthal GL, Ohye RG, Ghanayem NS, Cheatham JP, Tworetzky W, Martin GR. Hypoplastic left heart syndrome: current considerations and expectations. J Am Coll Cardiol. 2012; 59(1 Suppl):S1–42. [PubMed: 22192720]

3. Sedmera D, Hu N, Weiss KM, Keller BB, Denslow S, Thompson RP. Cellular changes in experimental left heart hypoplasia. The Anatomical Record. 2002; 267(2):137–145. [PubMed: 11997882]

4. Li F, Wang X, Capasso JM, Gerdes AM. Rapid transition of cardiac myocytes from hyperplasia to hypertrophy during postnatal development. Journal of Molecular and Cellular Cardiology. 1996; 28(8):1737–1746. [PubMed: 8877783]

5. Jopling C, Sleep E, Raya M, Marti M, Raya A, Izpisua Belmonte JC. Zebrafish heart regeneration occurs by cardiomyocyte dedifferentiation and proliferation. Nature. 2010; 464(7288):606–9. [PubMed: 20336145]

6. Bettencourt-Dias M, Mittnacht S, Brockes JP. Heterogeneous proliferative potential in regenerative adult newt cardiomyocytes. Journal of cell science. 2003; 116(Pt 19):4001–4009. [PubMed: 12928330]

7. Porrello ER, Mahmoud AI, Simpson E, Hill JA, Richardson JA, Olson EN, Sadek HA. Transient regenerative potential of the neonatal mouse heart. Science (New York, N.Y.). 2011; 331(6020):1078–1080.

8. Mollova M, Bersell K, Walsh S, Savla J, Das LT, Park SY, Silberstein LE, Dos Remedios CG, Graham D, Colan S, Kuhn B. Cardiomyocyte proliferation contributes to heart growth in young humans. Proceedings of the National Academy of Sciences of the United States of America. 2013; 110(4):1446–1451. [PubMed: 23302686]

9. Kuhn B, del Monte F, Hajjar RJ, Chang YS, Lebeche D, Arab S, Keating MT. Periostin induces proliferation of differentiated cardiomyocytes and promotes cardiac repair. Nature medicine. 2007; 13(8):962–969.

10. Williams C, Quinn KP, Georgakoudi I, Black LD 3rd. Young developmental age cardiac extracellular matrix promotes the expansion of neonatal cardiomyocytes in vitro. Acta biomaterialia. 2014; 10(1):194–204. [PubMed: 24012606]

11. Borgens RB. The role of natural and applied electric fields in neuronal regeneration and development. Progress in clinical and biological research. 1986; 210:239–250. Journal Article. [PubMed: 3960913]

12. Bentrup F, Sandan T, Jaffe L. Induction of Polarity in Fucus Eggs by Potassium Ion Gradients. Protoplasma. 1967; 64:254.

13. Cone CD Jr. Tongier M Jr. Control of somatic cell mitosis by simulated changes in the transmembrane potential level. Oncology. 1971; 25(2):168–82. [PubMed: 5148061]

14. McCaig CD, Rajnicek AM, Song B, Zhao M. Controlling cell behavior electrically: current views and future potential. Physiological Reviews. 2005; 85(3):943–978. [PubMed: 15987799]

15. Cone CD Jr. Tongier M Jr. Contact inhibition of division: involvement of the electrical transmembrane potential. Journal of cellular physiology. 1973; 82(3):373–386. [PubMed: 4590237]

16. Cone CD Jr. Cone CM. Induction of mitosis in mature neurons in central nervous system by sustained depolarization. Science (New York, N.Y.). 1976; 192(4235):155–158.

17. Sundelacruz S, Levin M, Kaplan DL. Depolarization alters phenotype, maintains plasticity of predifferentiated mesenchymal stem cells. Tissue engineering.Part A. 2013; 19(17-18):1889–1908. [PubMed: 23738690]

18. Blackiston DJ, McLaughlin KA, Levin M. Bioelectric controls of cell proliferation: ion channels, membrane voltage and the cell cycle. Cell Cycle. 2009; 8(21):3519–28.

19. Binggeli R, Weinstein R. Membrane potentials and sodium channels: hypotheses for growth regulation and cancer formation based on changes in sodium channels and gap junctions. Journal of Theoretical Biology. 1986; 123:377–401. [PubMed: 2443763]

20. Radisic M, Park H, Martens TP, Salazar-Lazaro JE, Geng W, Wang Y, Langer R, Freed LE, Vunjak-Novakovic G. Pre-treatment of synthetic elastomeric scaffolds by cardiac fibroblasts improves engineered heart tissue. Journal of biomedical materials research.Part A. 2008; 86(3): 713–724. [PubMed: 18041719]

21. Pai VP, Aw S, Shomrat T, Lemire JM, Levin M. Transmembrane voltage potential controls embryonic eye patterning in Xenopus laevis. Development. 2012; 139(2):313–23. [PubMed: 22159581]

22. Adams DS, Tseng AS, Levin M. Light-activation of the Archaerhodopsin H(+)-pump reverses age-dependent loss of vertebrate regeneration: sparking system-level controls in vivo. Biology open. 2013; 2(3):306–313. [PubMed: 23519324]

23. Blackiston D, Adams DS, Lemire JM, Lobikin M, Levin M. Transmembrane potential of GlyCl-expressing instructor cells induces a neoplastic-like conversion of melanocytes via a serotonergic pathway. Dis Model Mech. 2011; 4(1):67–85. [PubMed: 20959630]

24. Tseng AS, Beane WS, Lemire JM, Masi A, Levin M. Induction of vertebrate regeneration by a transient sodium current. J Neurosci. 2010; 30(39):13192–200. [PubMed: 20881138]

25. Sundelacruz S, Levin M, Kaplan DL. Depolarization alters phenotype, maintains plasticity of predifferentiated mesenchymal stem cells. Tissue engineering. Part A. 2013; 19(17-18):1889–908. [PubMed: 23738690]

26. Sundelacruz S, Levin M, Kaplan DL. Membrane potential controls adipogenic and osteogenic differentiation of mesenchymal stem cells. PLoS One. 2008; 3(11):e3737. [PubMed: 19011685]

27. Cone CD. The role of the surface electrical transmembrane potential in normal and malignant mitogenesis. Annals of the New York Academy of Sciences. 1974; 238:420–35. [PubMed: 4613241]

28. Adams DS, Levin M. Measuring resting membrane potential using the fluorescent voltage reporters DiBAC4(3) and CC2-DMPE. Cold Spring Harbor protocols. 2012; 2012(4):459–464. [PubMed: 22474652]

29. Adams DS, Levin M. General principles for measuring resting membrane potential and ion concentration using fluorescent bioelectricity reporters. Cold Spring Harbor protocols. 2012; 2012(4):385–397. [PubMed: 22474653]

30. Oviedo NJ, Nicolas CL, Adams DS, Levin M. Live Imaging of Planarian Membrane Potential Using DiBAC4(3). CSH Protoc. 2008; 2008:pdb prot5055. [PubMed: 21356693]

31. Engel FB, Hauck L, Cardoso MC, Leonhardt H, Dietz R, von Harsdorf R. A mammalian myocardial cell-free system to study cell cycle reentry in terminally differentiated cardiomyocytes. Circulation research. 1999; 85(3):294–301. [PubMed: 10436173]

32. Morgan KY, Black LD. Mimicking isovolumic contraction with combined electromechanical stimulation improves the development of engineered cardiac constructs. Tissue Eng Part A. 2014

33. Jenkins KJ, Correa A, Feinstein JA, Botto L, Britt AE, Daniels SR, Elixson M, Warnes CA, Webb CL, Y. American Heart Association Council on Cardiovascular Disease. Noninherited risk factors and congenital cardiovascular defects: current knowledge: a scientific statement from the

American Heart Association Council on Cardiovascular Disease in the Young: endorsed by the American Academy of Pediatrics. Circulation. 2007; 115(23):2995–3014. in the. [PubMed: 17519397]

34. Tseng A, Levin M. Cracking the bioelectric code: Probing endogenous ionic controls of pattern formation. Communicative & Integrative Biology. 2013; 6(1):1–8.

35. Levin M. Reprogramming cells and tissue patterning via bioelectrical pathways: molecular mechanisms and biomedical opportunities. Wiley Interdisciplinary Reviews: Systems Biology and Medicine. 2013; 5(6):657–676. [PubMed: 23897652]

36. Yang M, Brackenbury WJ. Membrane potential and cancer progression. Frontiers in physiology. 2013; 4:185. [PubMed: 23882223]

37. Swayne LA, Wicki-Stordeur L. Ion channels in postnatal neurogenesis: Potential targets for brain repair. Channels. 2012; 6(2):69–74. [PubMed: 22614818]

38. Aprea J, Calegari F. Bioelectric state and cell cycle control of mammalian neural stem cells. Stem cells international. 2012; 2012:816049. [PubMed: 23024660]

39. Yamada A, Gaja N, Ohya S, Muraki K, Narita H, Ohwada T, Imaizumi Y. Usefulness and limitation of DiBAC4(3), a voltage-sensitive fluorescent dye, for the measurement of membrane potentials regulated by recombinant large conductance Ca2+-activated K+ channels in HEK293 cells. Japanese journal of pharmacology. 2001; 86(3):342–350. [PubMed: 11488436]

40. Sachs HG, Stambrook PJ, Ebert JD. Changes in membrane potential during the cell cycle. Experimental cell research. 1974; 83(2):362–366. [PubMed: 4856272]

41. Young JL, Engler AJ. Hydrogels with time-dependent material properties enhance cardiomyocyte differentiation in vitro. Biomaterials. 2011; 32(4):1002–9. [PubMed: 21071078]

42. Liou JY, Hong HJ, Sung LC, Chao HH, Chen PY, Cheng TH, Chan P, Liu JC. Nicorandil inhibits angiotensin-II-induced proliferation of cultured rat cardiac fibroblasts. Pharmacology. 2011; 87(3-4):144–151. [PubMed: 21346392]

43. Quintas LE, Pierre SV, Liu L, Bai Y, Liu X, Xie ZJ. Alterations of Na+/K+-ATPase function in caveolin-1 knockout cardiac fibroblasts. Journal of Molecular and Cellular Cardiology. 2010; 49(3):525–531. [PubMed: 20451529]

44. Winnicka K, Bielawski K, Bielawska A, Miltyk W. Dual effects of ouabain, digoxin and proscillaridin A on the regulation of apoptosis in human fibroblasts. Natural product research. 2010; 24(3):274–285. [PubMed: 20140806]

45. Benamer N, Moha Ou Maati H, Demolombe S, Cantereau A, Delwail A, Bois P, Bescond J, Faivre JF. Molecular and functional characterization of a new potassium conductance in mouse ventricular fibroblasts. Journal of Molecular and Cellular Cardiology. 2009; 46(4):508–517. [PubMed: 19166858]

46. Fujio Y, Nguyen T, Wencker D, Kitsis RN, Walsh K. Akt promotes survival of cardiomyocytes in vitro and protects against ischemia-reperfusion injury in mouse heart. Circulation. 2000; 101(6):660–667. [PubMed: 10673259]

47. Shiojima I, Walsh K. Regulation of cardiac growth and coronary angiogenesis by the Akt/PKB signaling pathway. Genes & development. 2006; 20(24):3347–3365. [PubMed: 17182864]

48. Vaillant AR, Mazzoni I, Tudan C, Boudreau M, Kaplan DR, Miller FD. Depolarization and neurotrophins converge on the phosphatidylinositol 3-kinase-Akt pathway to synergistically regulate neuronal survival. The Journal of cell biology. 1999; 146(5):955–966. [PubMed: 10477751]

49. Liu L, Zhao X, Pierre SV, Askari A. Association of PI3K-Akt signaling pathway with digitalis-induced hypertrophy of cardiac myocytes. Am J Physiol Cell Physiol. 2007; 293(5):C1489–97. [PubMed: 17728397]

50. Harris IS, Zhang S, Treskov I, Kovacs A, Weinheimer C, Muslin AJ. Raf-1 kinase is required for cardiac hypertrophy and cardiomyocyte survival in response to pressure overload. Circulation. 2004; 110(6):718–723. [PubMed: 15289381]

51. Corvol JC, Valjent E, Toutant M, Enslen H, Irinopoulou T, Lev S, Herve D, Girault JA. Depolarization activates ERK and proline-rich tyrosine kinase 2 (PYK2) independently in different cellular compartments in hippocampal slices. The Journal of biological chemistry. 2005; 280(1):660–668. [PubMed: 15537634]

52. Maharana C, Sharma KP, Sharma SK. Feedback mechanism in depolarization-induced sustained activation of extracellular signal-regulated kinase in the hippocampus. Scientific reports. 2013; 3:1103. Journal Article. [PubMed: 23346360]

53. Tahara S, Fukuda K, Kodama H, Kato T, Miyoshi S, Ogawa S. Potassium channel blocker activates extracellular signal-regulated kinases through Pyk2 and epidermal growth factor receptor in rat cardiomyocytes. Journal of the American College of Cardiology. 2001; 38(5):1554–1563. [PubMed: 11691539]

54. Xie Z. Molecular mechanisms of Na/K-ATPase-mediated signal transduction. Annals of the New York Academy of Sciences. 2003; 986:497–503. Journal Article. [PubMed: 12763870]

a) Original cardiac α-actin image.
b) Thresholded cardiac α-actin image.
c) Overlay the mask on nuclear stain image.
d) Count the nuclei within masked regions.
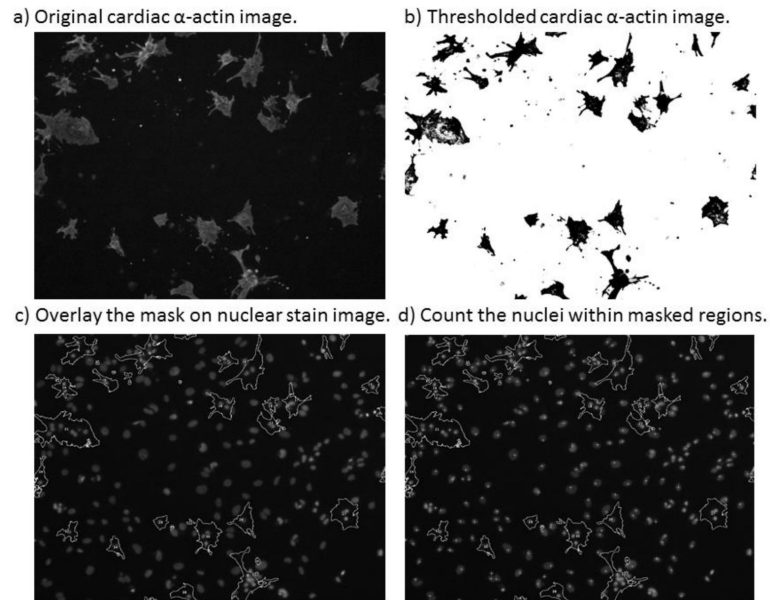
Figure 1.
Demonstration of the steps of microscopic cytometry. A fluorescent image of one of the cultures labeled with antibodies against cardiac α-actin (a). This image is then thresholded to create a binary mask (b), which is overlaid on the Hoechst nuclear stain image of the same region of the culture (c) and the nuclei within the masked regions are counted to determine the CM number (d).
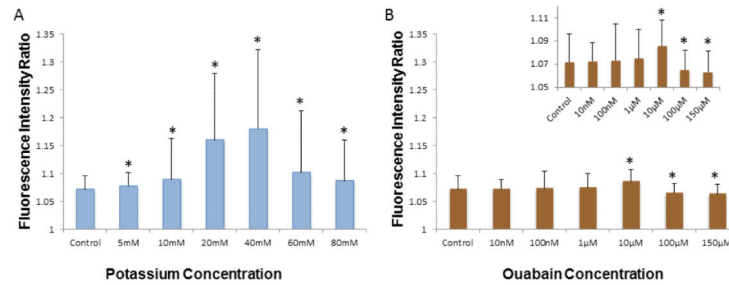
Figure 2.
Fluorescence intensity ratio calculated from DiBAC(4)3 fluorescence staining demonstrating the depolarizing effect of a) potassium gluconate, and b) ouabain. The inset shows, a scale-adjusted graph to emphasize the difference between groups. Note that a higher ratio indicates a more depolarized membrane potential (Mean±SEM. Minimum 149 cells per conditions, $p < 0.001$ among treatment, * $p < 0.05$ compared to control group by one way ANOVA)
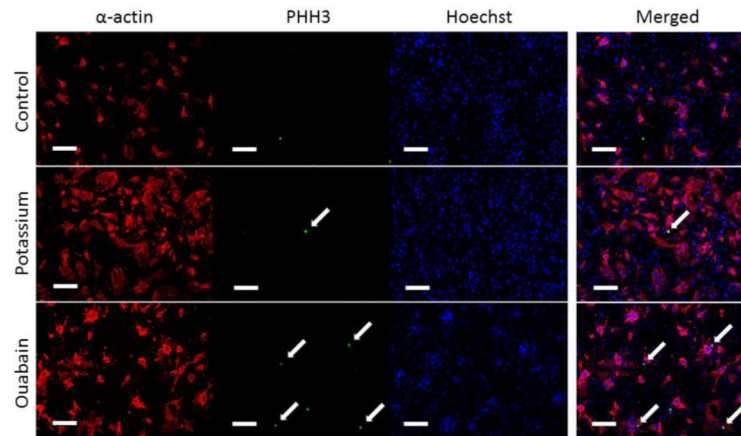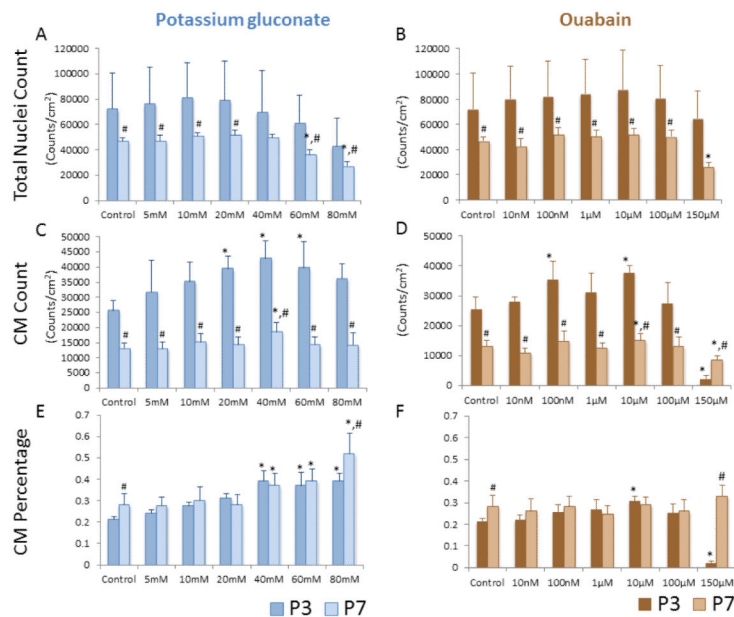
Figure 3.
Representative images of sarcomeric α-actin (red), PHH3 (Green), Hoechst (Blue) for control P3 cardiac cell cultures and P3 cultures subjected to 40 mM potassium gluconate or 10 μM ouabain. Merged images for each of the three groups are shown on the right. The white arrows denoted proliferating cells indicated by the PHH# positive nuclei. Scales bar equal 100 μm in all images.

Figure 4.
Total nuclear density for potassium gluconate and ouabain. CM density as measured by sarcomeric α-actin positive cells for potassium gluconate (c) and ouabain (d). CM percentage for potassium gluconate (e) or ouabain (f). Data from P3 cells is shown in the darker color bars, while data from P7 cells is displayed in the lighter color bars. (*p<0.05 among treatment compare to control, ANOVA; #p<0.05 comparison between P3 and P7 cells at the same treatment).
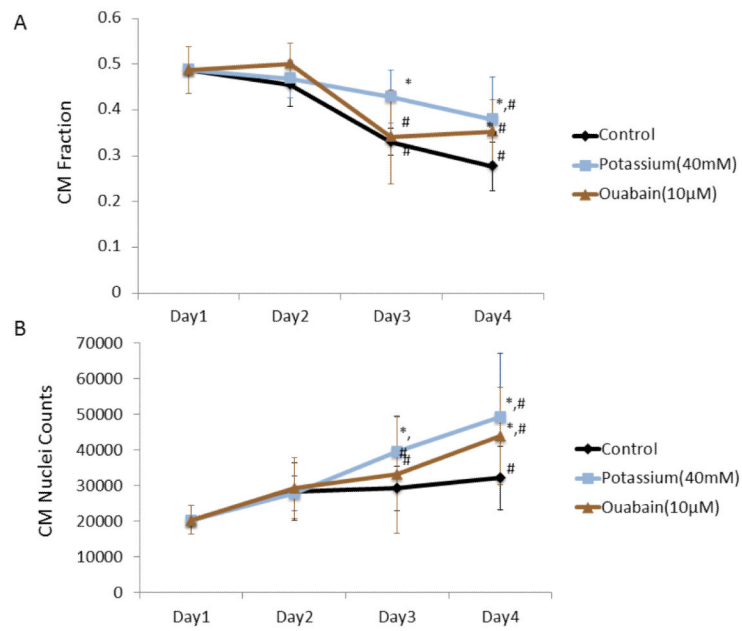
Figure 5.
Growth curve for four days culture. CM percentage for optimal conditions in potassium gluconate and ouabain (a). CM nuclei counts for optimal conditions in potassium gluconate and ouabain (b). (*p<0.05 among treatment compare to control, ANOVA; #p<0.05 compared to day 1)
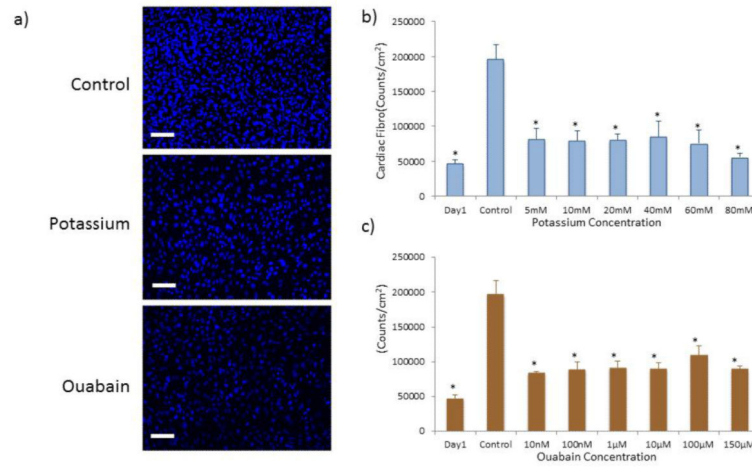
Figure 6.
a) Representative images of Hoechst nuclei stain of P3 CFs in control conditions (top) as well as after treatment with 40 mM potassium gluconate (middle) and 10 μM ouabain (bottom). Nuclei count of CF at varying concentrations of b) potassium gluconate and c) ouabain. (*p<0.05 as compared to control group, ANOVA).
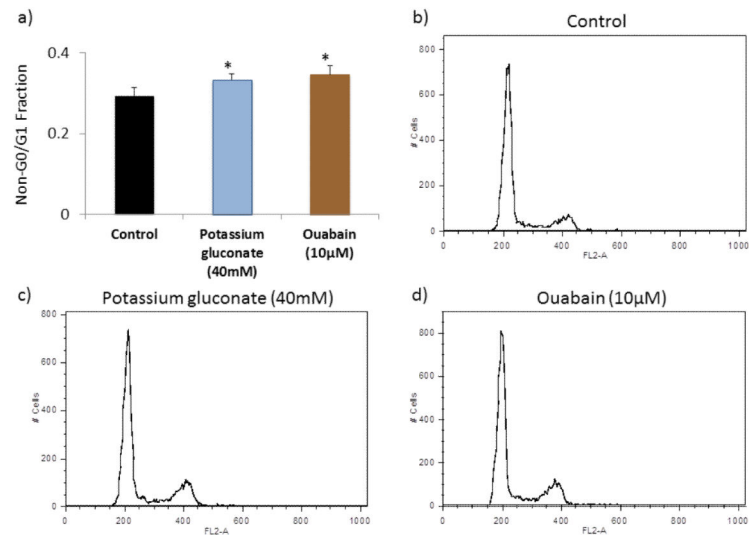
Figure 7.
Cell cycle analysis in P3 populations carried out by flow cytometry on cells labeled with propidium iodide. (a) Non-G1/G0 cells percentage in each group. (*p<0.05 compared to control group, n=4, 10000 counts per sample, ANOVA). FL-2A channel histogram for (b) control group, (c) 40mM potassium gluconate, (d) 10μM ouabain.
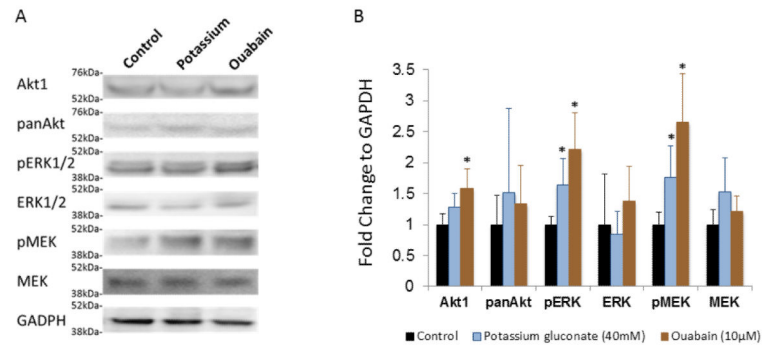
Figure 8.
a) Representative Western blots of Akt1, pan Akt, pERK1/2, ERK1/2, pMEK, MEK, and GAPDH of control cultures of P3 cardiac cells as well as those subjected to the two depolarization treatments at the optimal concentrations. b) Quantification of Western blot derived expression, normalized to control conditions. * denotes p<0.05 compared to control condition.